EXPERIMENTAL INVESTIGATION FOR STRENGTHENING THE NANOCOMPOSITE CEMENTITIOUS MATERIALS WITH ANANOSCALE MODIFICATION

Arpita Das*, Showmen Saha

*Arpita Das, Ph.D. student,NIT, Durgapur, Mahatma Gandhi Rd, A-Zone, Durgapur-713209, West Bengal, India.ORCID ID - 0000-0002-6870-6101 ph:9831356955 Email id- ad.16ce1304@phd.nitdgp.ac.in

Showmen Saha, Professor,C.E. department,NIT, Durgapur, Mahatma Gandhi Rd, A-Zone, Durgapur- 713209, West Bengal, India, ph: 9434788008, Email-id – showmensaha@gmail.com

Abstract: For the last few decades,researchers have widely used nano polymer to control the mechanical properties of cementitious materials as a micro reinforcement.This paper examines and compares the mechanical and microstructure property of nanofiber cementitious material. Twenty-four sets of beam/cube cast withCNFs cementitious material where CNFs were used from 0.1%, 0.2%, and 0.3% of cement weight. The nanoparticles were scattered using surfactant and an ultrasonic probe sonicator and then cast in different types of moulds. The 28-day compressive and 3-point flexure bending strength was tested. As a result, properties like flexural strength, Compression Strength,Young's Modulus, Toughness, and strain capacity of various percentages of CNFs cementitious materialwere estimated. 3-point flexure bending strength test, flexural strength, Compression Strength,Young's Modulus, Toughness, and strain capacity were estimated of every CNFs nanocomposites.Increasing the percentage of CNFs, flexural strength improved by 43%,65%, and 68% compared to without nanofiber cementitious material, enhancing its toughness and young modulus. SEM and TEM result was observedto understand proper bonding between nanofiber and cementitious material.The XRD results were used to analyze thephase identification, crystalline size, crystallinity index(CI), and d-spacingfor all sets of cementitious materials. FTIR results were also introduced in this paper to identify the board peaks that facilitate the functional group's electron delocalization pattern.After completing this study, the microscopic and mechanical analysis may offer a key reference for carbon nanofiber cement composites, which can lift their strength, constancy, integrity, densify and reinforce the composite microstructure.

Keywords: Carbon Nanofibers, Cement, 3 points flexural bending strength, Rheological properties, SEM results, XRD results.

Introduction:

The use of cement and cementitious materials in construction is very much widespread nowadays. However, the value of the tensile strength of concrete was very much low. Therefore,it was required to provide some reinforcement to enhance flexural strength, ductility, and toughness.Over the past few decades, the researchers have introduced. Not only that, the Nanofiberswere used as an energy-saving material; with the addition of some Nanofibers in building materials, the buildings were going to be more durable and economical. The cost of nanofibers was relatively higher, but their total strengthwas much higher than other reinforcing materials.Carbon Nanofibers (CNFs) were rapidly flattering most popular cementitious materials. It has excellent mechanical, electrical, and thermal conductivity. CNFs can be transmittedinto various metals, i.e., elastomers, ceramics,thermoplastics, thermosets. Introducing nanofiber in a concrete beam without stirrup could resist crack propagation(Altoubat, 2009).The nanofibers or polymer application in a different surface facilitates the various surface techniques modification. They were dispersed in isotropic and anisotropic solutions. As they were made with carbon atoms, they were used in the strengthening process. The interlaminar region of Carbon nanofibers improves the properties of composites for different applications.(S. R. Dhakate et al., 2016)The chemical vapor deposition of Carbon Nanofiberswas producedby Vapor-grown Carbon Fiber (VGCNF), from which the nanofiber dispersion, alignment, bond between nanofibre and polymer, mechanical properties were described by Mohammed H.Al(Mohammed H. Al-Saleh, 2009).VGCNF hadexcellent mechanical properties. The thermal stability was very high,giving high strength and ductility in high temperatures and reducing the crack if clay was coated with CNF composite.(Mohammed H. Al-Saleh, Uttandaraman Sundararaj, 3. December 2011)There was another type of carbon Nanofibers, i.e., Graphitic Carbon nanofibres (GCNFs), which were produced with some aligned electrospun polyacrylonitrile (PAN) Nanofibers. As per Zhou, Z. P. et al. in 2009, these electrospunpolyacrylonitrile Nanofibers consist of phosphoric acid, which enhances the thermal, mechanical, morphological property of graphitic carbon Nanofibers. The mechanical strength increased 62.3% than the precursor nanofibres without phosphoric acid(Zhengping Zhoua, Chuilin Laia,b, Lifeng Zhangb, Yong Qiana, Haoqing Houa,*, Darrell H. Renekerc, Hao Fongb,**, 2009). This type of graphitic carbon Nanofibers was used in the stabilization process. The thermal stability and mechanical stability were also high, and was mechanical stability was coming from the microporous ceramic structure of CNFs. In the case of morphological property, the best growth of CNFswasachieved whenan essential amount of nickel nitrate hexahydrate Ni $(NO_3)_2 \cdot 6H_2O$mixed with a small quantity of acetone (Panel Muneer et al., 2015).The mechanical stability of CNFs was raised by internal walls, which werebuilt by the microporous ceramic structure. This ceramic structure also helps to produce porous material. Carbon nanostructureswithporous ceramicinternal walls produce to determine a set of growth of pore size around 25μm. Mainly there were two steps, first the nanostructure transfer inside of the scaffold. Using an iron catalyst, the chemical vapour of

nanofibrewas deposited into the scaffold, and the growth process started. After the growth process, the catalyst remains in the framework.ClaudiaWalter, in 2013 investigated scaffolds made by alumina, which was a help to the growth of nanofiber under the scaffold.Nanofibers were also used as a cementitious material to improve the performance of saving energy. F. Scalwasi, in 2008 used Nanofibers as a less energy conservator; as a result, insulation or lighting of a new or old type of building without damage of any building(Scalwasi, 2009).(F. Scalwasi, 2008).Some fibers were also used as heat insulation polyurethane foam. M. M. Alavi Nikje et all. In 2008 also described achieving best dispersion condition 3-aminopropyltriethoxysilane (APTS) to be used as a coupling agent and to use it thermal, mechanical, and dynamic behavior was going to be enhanced(Mir Mohammad Alavi Nikje, 2008).Mejdoub R et al. in 2016 were described Thermal, mechanical and microstructural properties when Nano fibrillated cellulose used in nano reinforcement in Portland cement. (Mejdoub R et al., 2016). To increase processability, good dispersion stability was required. For that, the resultant hybrid composites were tested, and it shows, the CNFs were much lesser than the electrochemical specific capacitance of the CNFs.(Du, 2012).As perYehya M. Ahmed, at 400ºC to 570ºC, the surface area of nanofiber increased with the increase of zeta potential(Yehya M. Ahmed, 2016).In this study, TEM results were used to determine the sonication time, but these examinations also confirmed the shorter CNFs were more stable than longer ones. TEM also analysesbamboo-like herringbone composite structures whereCNFs have grown vertically (I. Teng, 2012).To investigate XRD results, many researchers considered the Segal equation. Based on the Segal equation, the crystallinity index of the Cellulose nanofiber with diameters 50 to 100 nm,having 72% crystallinity index.Cellulose nanofiber has higher thermal stability than lignin, associated with the high crystallinity of CNF(Gea, 2020).First, the material dried and got into a powder form for an XRD result, and then the other property like temperature, acid concentration, mechanical treatmentwasperformed(Das K. R., 2009).After getting all properties, crystallinity and d-spacing were found out.(D. J. Bannwaster, G. R. Davies, I. M. Ward, and J. F. McIntyre, 1984).

Fourier Transform Infrared (FTIR) spectroscopy was also used in this paper to determine the chemical structure of materials and compounds. It is used for both qualitative and quantitative analysis to identify the functional groups attached to the structure of materials. The main structure of a compound is determined by infrared (IR) energy absorbed by its chemical bonds and at the definite wavelength (frequencies). The strength and amount of chemical bonds present in the compound can be mapped through the IR absorptions at specific spectral locations.

The above-conferred studies discussed the property of various types of carbon nanofiber.How CNFsdispersed in solutions and resisted the crack propagation using coating by nanofiber. Although the researchers introduce enhancement of mechanical properties, there are many research gaps. Firstly, proper process technique, sonication time-related problem,

percentage variation of CNFs with various models for proper bonding, and consistent improvement of properties. Secondly, the microscopic physical parameter, i.e., phase-identification, crystalline size, crystallinity index, d-spacing,need to be utilized to explain their effect on carbon nanofiber cementitious material. Thirdly, the chemical behavior, i.e., peak values IR response, observed thefunctional group's electron delocalization. From the past research gaps, the objective of the present study is to establish an essential understanding between CNFs and cementitious material with variable percentages of CNFs. The study report is blended with the physical, chemical, and mechanical behavior of the CNFs cementitious material.

Materials and Methods

Materials

In this study, Portland cement of grade II was used to prepare the experimental model, and the cement test wasfinished to get the properties of cement. A graphitized(iron-free) composed of conical platelets CNFs were used in this study, which has anaverage diameter of 130nm and length varies from 20 µm to 200 µm. It was an iron-free content having a pore size of 0.075 cm^3/g of the average pore volume. The cement and CNFs were not the same, so they were not immersed in water only by hand mix. Due to the various graphitic and compatible properties, the CNFs dispersed in the anisotropic and anisotropic matrix.The graphitized CNFs were dispersed into water by using some superplasticizers. N, N-Dimethylformamide (DMF) was used to disperse the CNFs in a cement matrix with a minimum time.After dispersed into the solution, the ph value of dispersion water was observed.The properties of Carbon Nanofibers were taken from Sigma-Aldrich from where carbon Nanofibers were ordered. The property of CNFs was discussed in "Table 1".

Table 1: Properties of Carbon Nanofibers

Diameter (D)	$100nm$
Length (L)	$30\ \mu m$
Avg Dia	$130nm$
Average specific surface area	$24 m^2/g$
Average bulk density	$2\ lb/cu.ft$
Purity (wt%)	>90

Methods

Twenty four beam/cube casted in this study.Among them, the eighteen sets were mixed with CNFs at 0.1, 0.2, and 0.3 percentage of the weight of cement with large and small beam sizes, and six sets were for reference with a different dimension of cementitious material. These eighteen sets were summarized in "Table 2".There were two types of beam one type represents a large, and another type represents a small beam. The length and cross-section of the large beam were 400 mm and 14mm × 14 mm,respectively, whereas the length and cross-section of the small beam were 160 mm and 6.5 mm × 6.5 mm."Table 2(a)" representsa large type beam, and "Table 2(b)" represents a small type of beam. In every set, three no beams were cast for 3 point flexure bending strength test, and three no cubes of dimension 50mm × 50mm ×50 mm were cast under each set for getting the compression test result. As per Nur Yazdani in 2016, 0.35 to 0.4 water-cement ratio gives the higher strength(Yazdani, Nur & Mohanam, Vinoth, 2014).In this study, it was taken for every set of the sample was 0.4as 0.4 water-cement ratios more workable than 0.35. N, N-Dimethyl formaldehyde was used as a surfactant to mix with the water where the water to surfactant ratio was 0.005.(Bryan M. Tyson, 2011).An aqueous solution was prepared by mixing water, surfactant, and CNF. The pH of the aqueous solution was measured by a pH meter, and the ranges were 8.2-8.4. After measuring pH value, the solution was sonicated for 30 min using an ultrasonic sonicator (model F.S. – 750, frequency 23 ± 3 KHz) as shown in "Figure 1". The sonicated time was dependent upon theTEM results. When the sonication time was 15 min, there some black spot was visible. Remove the black spots on thesample, the sonication time

Table 2(a): Description of Large sample of beams

Specimen Title	Specimen Description	Water-cement ratio	Percentage of CNFs
SET 1	Large beam(400 mm × 14 mm × 14 mm)	0.4	0
SET 3	Large beam (400 mm × 14 mm × 14 mm)	0.4	0.1
SET 4	Large beam ((400 mm × 14 mm × 14 mm)	0.4	0.2
SET 5	Large beam ((400 mm × 14 mm × 14 mm)	0.4	0.3

Table 2(b): Description of Small sample of beams

Specimen Title	Specimen Description	Water/cement ratio	CNFs (% weight of dry cement)
SET 2	Small beam (160mm × 6.5mm × 6.5mm)	0.4	0
SET 6	Small beam (160mm × 6.5mm × 6.5mm	0.4	0.1
SET 7	Small beam (160mm × 6.5mm × 6.5mm	0.4	0.2
SET 8	Small beam (160mm × 6.5mm × 6.5mm	0.4	0.3

was improved, and after 30 min sonication, the black spots were removed. When sonication was complete,the dispersed solution was mixed with cementitious material. A multispeed planetary mixer was

Figure 1: Sonication by ultrasonic sonicator

Figure 2: After casting the sample (cube and beam specimen)

used for 13 to 18 min to increase the evenness of the matrix. Before moulding, for removal of an air bubble, the even sample was rest 4 to 6 min in a vacuum chamber. After that, the sample was placed into wooden moulds with a cross-section of 6.5 mm × 6.5 mm and 14 mm × 14 mm and also poured into the cube mould with a dimension of 50mm × 50 mm × 50 mm as shown in "Figure 2".An electric surface vibrator was used to fill the embedded air voids. After 24 hours, all samples were de-moulded and kept in saturated lime water for curing for 28 days.X-ray diffraction patterns were also considered here. A Miniflex Desktop X-ray DiffractometerRigaku, with a Cu Target and having radiation at 30 kV and 15mA. The Scanning Range was ~ 30 ~ +1500 (2q), and the Scanning speed was 0.010 ~ 1000/min. After 28 days some powder sample was prepared for each type set for XRD result. In this paper, some samples were prepared to investigate the SEM image. Very thin specimens of all samples were prepared, and after coating with silver wrapping, the samples were placed in a Scanning electron microscope. This paper used the SHIMADZU IRPRESTIGE-21 model (installed in

CMERI Durgapur) for diffuse reflectance spectroscopy. The scan range of this model is 400nm-4000 nm Wave Length-nm-1. As per Fuller and Griffiths description of diffuse reflectance, the technique is utilized here. The sample was scanned multiple times with a resolution of 2.0 cm− 1,and the presented data is an average value. Each sample was prepared and analyzed three times, and the final spectrum was an average of these three measurements to minimize differences due to sample preparation. After preparation of sample wasplaced in the sample holder of the DR-FTIR spectrometer.

Experimental setup:

In this study, two types of specimen one cube specimen for conduct compression strength test and another beam specimen for conduct flexural (3-point bending strength) test. The compression test was done by Universal Testing Machine made by HEICO shown in "Figure 4". Flexural strength test was done by three-point bending strength test machine (H50KS by TinueOlasen)installed in CMERI Durgapur shown in "Figure 3". An excel sheet was prepared from the test result. From the strength of material relation, these data were converted to stress-strain, i.e., stress $\sigma = \frac{3pL}{2bd^2}and\epsilon = \frac{6Dd}{L^2}$, p was the force from a load cell, L = span length(Bryan M. Tyson, 2011)[Here, for a Large beam length = 400 mm and a small beam length = 160 mm], b = width and d = depth [for large beam 14 mm X 14mm and small beam width and depth was 6.5mm X 6.5mm] and D was the corresponding displacement.Scanning Electron Microscopic(SEM) results were taken for every sample to observe the bonding properties between cement paste and CNFs. To follow the surface crack of

Figure 3: 3 point bending strength test by H50KS by TinueOlasen

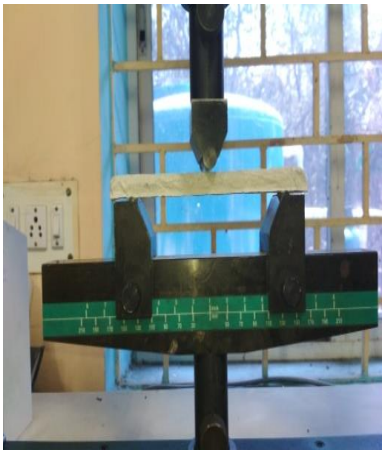

Figure4:Compressionstrength testing machine

the sample,a Scanning Electron Microscope (S-3000N) with a high resolution was used. A fracture surface was cut approximately3 × 3 × 1 mm from every set of samples for SEM sample and three nm thick palladium layer coated with the surface toenhance surface conductivity. Suppose the coating was not implemented to the surface of the SEM sample. In that case, the results or image could not be generated because the cement was not conductive material, so the electron had not reached the surface of the materials.(Nur Yazdani, Vinoth Mohanam, 2014)

Result and Discussion:

Aqueous Solution:

Transmission Electron Microscope image was considered for the different types of sampleto find out the sonicatedtime inthe ultrasonic mixture, whether it was dispersed correctly or not. In "Figure5,"the sonication was done for 15 min, and it was seen that after 30 min sonication with 1.25 % surfactant by weight of the water,it gave better results,and all-black spots were removed.

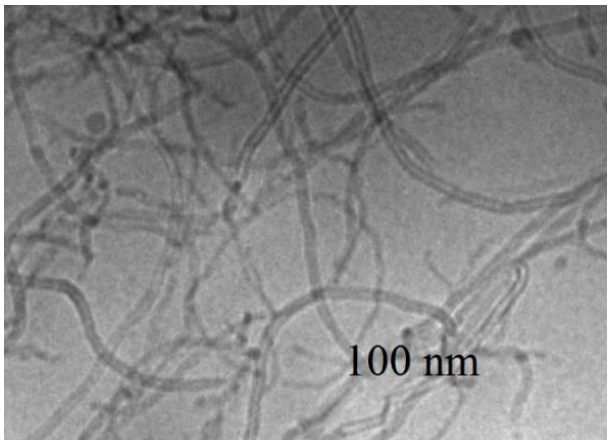

Figure5dispersion of CNFs in aqueous solution after 30 min sonication

Mechanical Properties:

Flexural strength and compressive strength were done for 7,14 and 28 days to find out the mechanical properties. The size of the cube mould and the water-cement ratio as described in "Table 3". The peak load was considered for the compression strength test, and a bar chart was followed as per "Figure 6".Here the bar represents the peak value of compressive strength with time. In "Figure 7"., itwasobserved that at first, CNF improves the peak loadand peak displacement of cement paste, but at a certain percentage, the peakdisplacement was decreed with an increase of CNF % with cement. It was also observed that the increase in strength was minor for increasing nano filament for compressive strength. Eight sets of the beam were cast for bending strength, and after 7, 14, and 28 days, the 3 point bending strength results were observed.As the ultimate strength gains in 28 days, so here 28 days bending strength results were considered.

The results are shown in "Figure 8". Here,two types of beams(long and short type of beam) was considered, and in both the case increase of nanofibre up to 0.2% increased the strength (set 1 to set 4 and set 6 to set 7) and for set 5 and set 8

Table 3: Description of Cube sample for compressive strength Test

Specimen Title	Cube Specimen Description	Water/cement ratio	CNFs (% weight of dry cement)
CementitiousMaterial Only	50 mm	0.4	0
With 0.1% CNF	50 mm	0.4	0.1
With 0.2% CNF	50 mm	0.4	0.2
With 0.3% CNF	50 mm	0.4	0.3

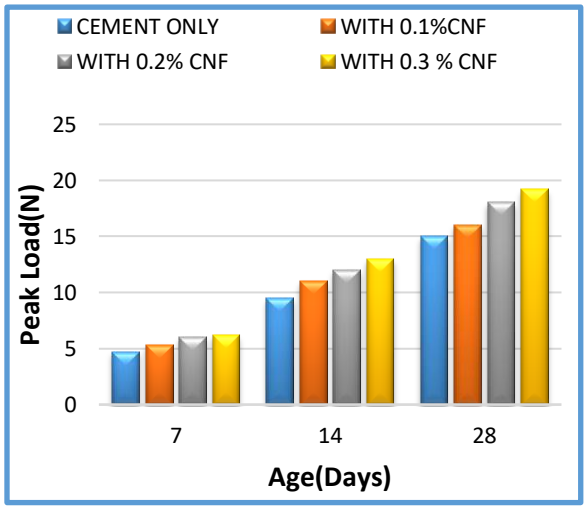

Figure 6 Peak load effect with or without CNFs

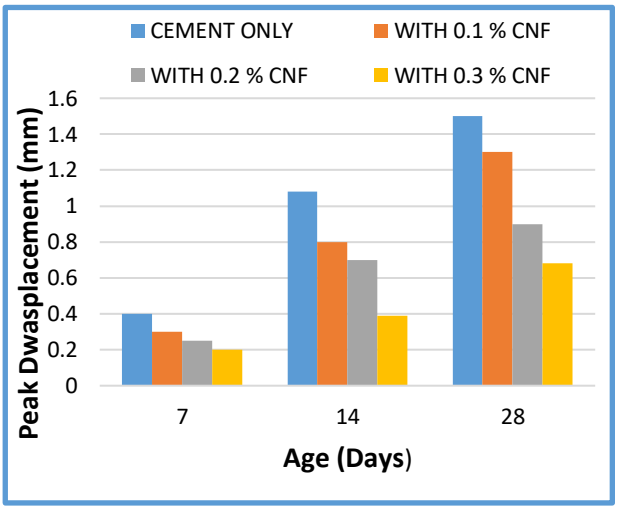

Figure 7. Peak displacement effect with or without CNFs

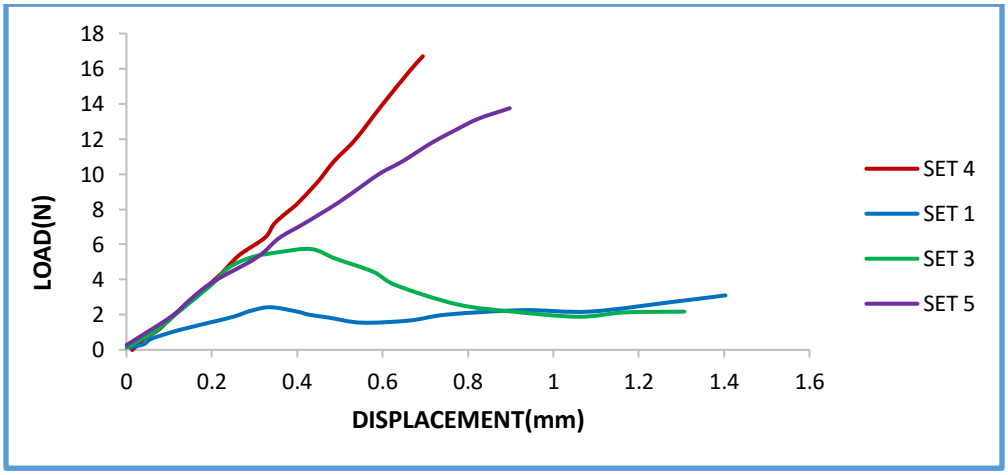

Figure 8 (a): Load displacement response of 3- point bending strength test of Large Beam sample at 28 days

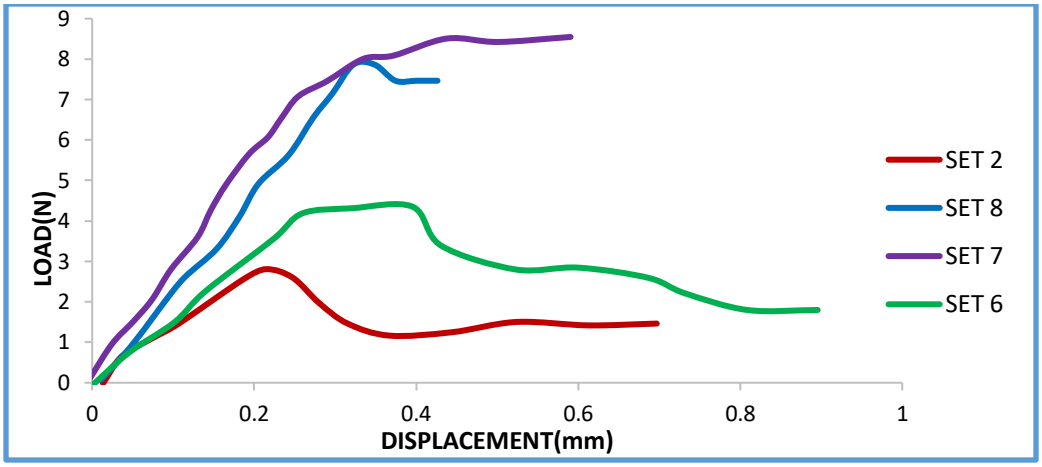

Figure 8 (b): Load displacement response of 3- point bending strength test of small beam sample at 28 days

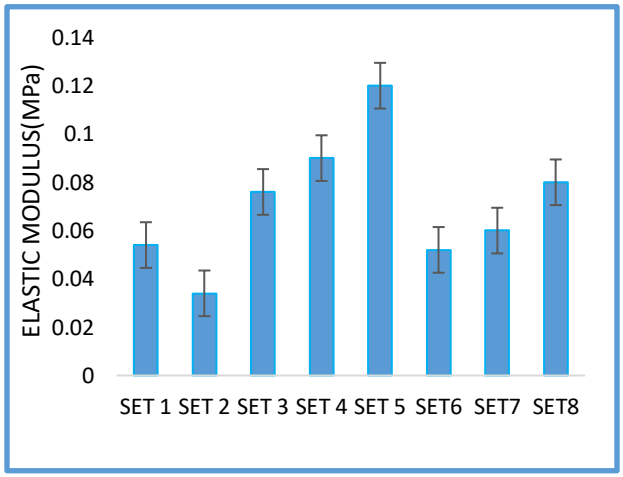

Figure9: Elastic modulus of cement paste

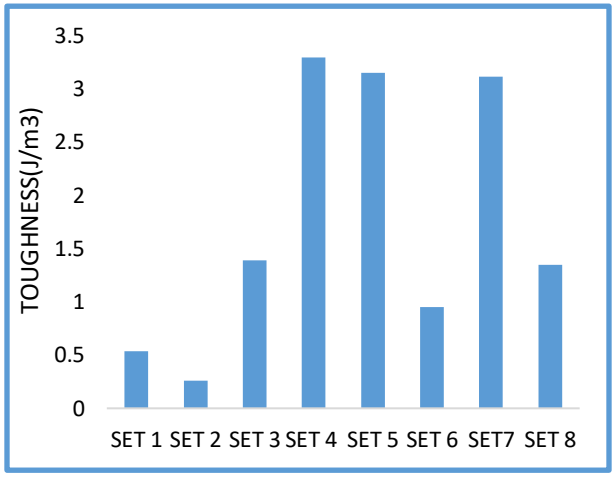

Figure10: Toughness of cement paste

bending strength was decreased. As a result, the bending strength was increased up to a certain percentage, but it decreased after that. "Figure 9" represents the elastic modulus of various sets of cement paste, and here it noticed that increasing the percentage of carbon nanofibers, the elastic modulus also increased for both large and small beams. Using MATLAB 2019a, the toughnessfind out from the stress versus strain curve."Figure 10" represented the toughness of all sets of all samples. In this case, the toughness of set 5 and set 8 types of the beam were relatively less than the other sets of cement paste. A certain percentage of increased nanofiber the load-bearing capacity were reduced due to that the toughness also decreased.

SEM Observation:

The TEM result was observed to know the proper mixing of nanofiber in an aqueous solution, but after blending up the solution with the cement matrix, the poor dispersion was shown in SEM results.(Viet, 2007) In "Figure 11", the aqueous

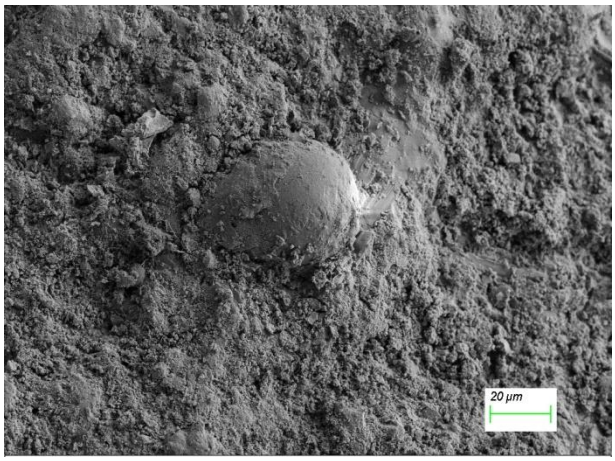

Figure 11: SEM image of hand mixing cement paste (without CNF)

Figure 12: SEM image of CNF embedded with Cement matrix (mixed with multispeed planetary mixer

solution was mixed with cement matrix by hand mixing, and as a result, the lumps were generated after the hydration of cement. In "Figure 12", the cement matrix was mixed with a multispeed planetary mixer with 0.2 % CNF, and as a result, the lumps were not generated, and CNF was also mixed up properly. After enlarging the SEM image, it was observed that a microcrack wasgenerated ("Figure13") in a specific region where the concentration of CNF was present. It was happened due to the weak binding of CNFs in a cement matrix. At the time of hydration, after hardening the cement hydrate outer surface to the inner surface of the sample, so the hard surface whereas grains hydrated in the absence of CNFs and prepared C-S-H without any CNFs, but when the CNFs was present, the areas were much more significant than individual grains of cement, in that case, the cement were clumped together, and as a result, cracks were generated. The Dispersion of cementitious material was described by Yazdanbakhsh et al. (2009) (Yazdanbakhsh, A, 2009). Here"Figure 14", the microcrack was generated, and the presence of Carbon Nanofibers was triedto pullthem out.

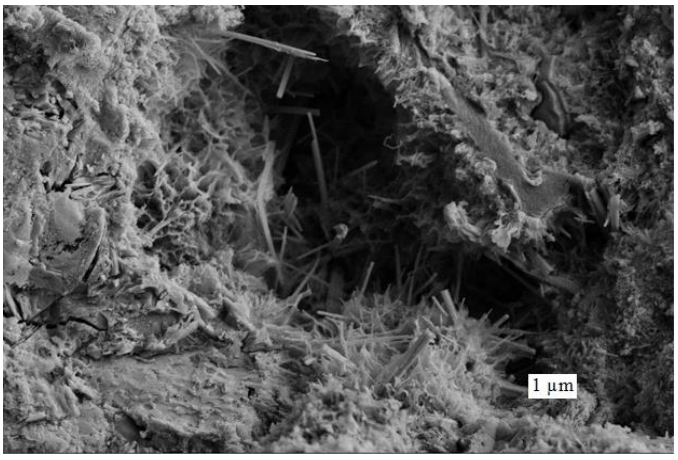

Figure:13SEM image for micro cracked fractured surface

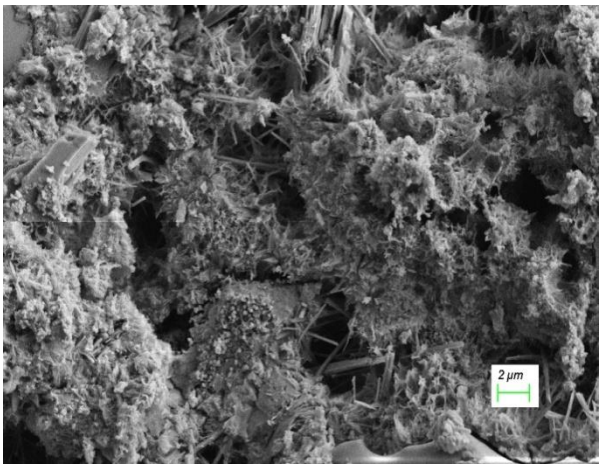

Figure 14Pulled out from a microcrack"Figure 14" shows a microcrack pulled out by CNF,i.e., other surfaces pulled one surface, and it was widespread in SEM images.

Due to untreated nano filament having a smooth surface, so the bond strength was not generated properly. As a result, due to the weaker bond, some microcracks were not resolved to increase the percentage of CNFs.

XRD Results:

XRD results were performed for all samples to investigate the phase identification. The dried powder from all samples was prepared for theXRD analysis."Figure15" showed the corresponding diffraction pattern ofcementitious material. Hydration products also showed, including SiO_2 and$CaCO_3$. The SiO_2 and $CaCO_3$, and CNFs data matched with 26.7019, 29.475, 30.217, 43.005, based on JCPDS, respectively. JCPDS match software was introduced, and the phase identification of sample powder diffraction was made. "Figure 15"display that crystalline graphiteinterlayer in $2\theta = 20–50°$. Inthe case of cement, there some changes occurred, and this interlayer $2\theta = 25–48°$. XRD diffraction results of cement sample were shown in"Figure 16," and here was for cement sample, and it could be easily stated that the no of peaks was turned less than cement with nanofiber sample and here match data had coincided the reference data at 26.67,34.33 and 46.77. This indicated that the presence of carbon layers increases the no of peak and also the value of 2-theta and revealed encapsulated iron. After Analysis of XRD peak profiles of cement and CNF cementitious materials, it can be said that the FWHM means full-width at half-maximumwas also effective for measuring sensitiveness in stress-strain built up andmicrostructure in the material. Here FWHM value of CNF increases more rapidly than FWHM values of cement, and as per H.M. Tung et al., a Linear decrease of FWHM in the XRD peak represents increases in density and hardness, and it also decreases the crystallinity(Mejdoub R, 2016).

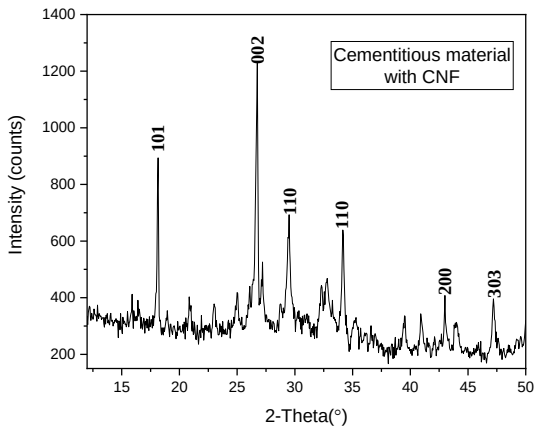

Figure 15:XRD Peak results for cement with CNF

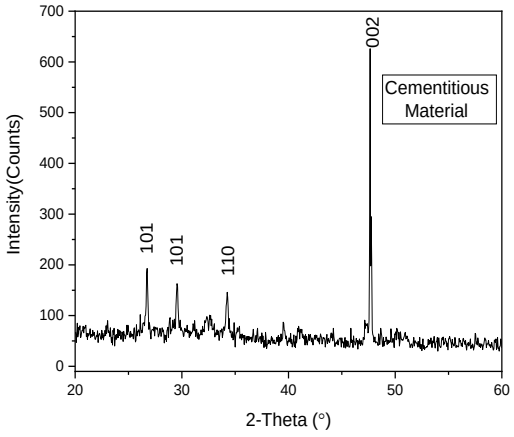

Figure 16:XRD Peak results for cement. The

XRD pattern of CNF cementitious material and cement was shown in "Figure 15" and "Figure 16", respectively. Using the Scherrer equation, the crystallite sizewas calculated from XRD graphs(Das K. &., 2010)

$$L_{h,k,l} = \frac{K\lambda}{\beta COS\theta}$$

Where K = 0.9 and λ = 1.5418Å (Mondragon, 2014)based on the FWHM value of 101 and 002 reflections. The crystallinity percentage was also calculatedusing the equation below.

$$\%\, Crystallinity = \frac{I_{002} - I_{am}}{I_{002}} \times 100$$

Crystallite sizeand crystallinity index values for all sampleswere described in Table 4(Thien Duc Nguyen Van S. S., 2014).This was based on the perpendicular plane of 002, 101. The Crystallinity of CNFs cementitious material was also increased due to the decrease of amorphous fractions. The XRD gives more information onthe interlayer of existing

Table 4: D-spacing, crystallinity Index, Crystal Size of various sample

Sample	CNF	Cementitious Material	Cementitious material with 0.1% CNF	Cementitious material with 0.2% CNF	Cementitious material with 0.3% CNF
d-spacing of the plane	0.387	0.403	0.393	0.384	0.384
Crystallinity Index(CI)	88	56	67	72	79
Crystal Size perpendicular to the plane	15.57978	3.869799181	4.888924872	5.266741573	9.747869988

elements and graphite in each sample. The CNFs matched with data JCPDS data(Thien Duc Nguyen Van S. S., 2014).FromFigure 15, it was observed that the d-spacing interlayer of crystalline graphite was not changed in 2θ = 20–30º. The crystallinity index was increasedwhen the percentage of CNFs cementitious material increased as the amorphous phases were present in a regular cement matrix.

FTIR Results:

Fourier transform infrared (FTIR) analysis results of with or without CNFs nanocomposites particles were shown in Figures 17 to 19. After preparing a sample, Infrared radiation was absorbed in various wavelengths, and the molecular composition was generated. Due to a change in the chemical structure, there was a change in the peaks after the heating process. The the figureshows the change of FTIR peak and pattern. In short, since IR is vulnerable to heat, this should be the decomposition of organic components into carbon material. The FTIR peak was changed when the temperature was

higher than 180°C. (Nandiyanto, 2017). The performance of IR response was feeble for carbon materials. Fig 17 to 19 represents the FTIR spectra of the various percentage of cementitious material. The graph reveals the shift of characteristic peaks from 450 cm^{-1} to 3800 cm^{-1}.The FT-IR spectra of hardened cement pastes were compared with some percentage of CNFs at 28 days of hydration. The wideband was observed in the region 1355, 2068, 2256, 2942 cm−1 is caused by C-O, the

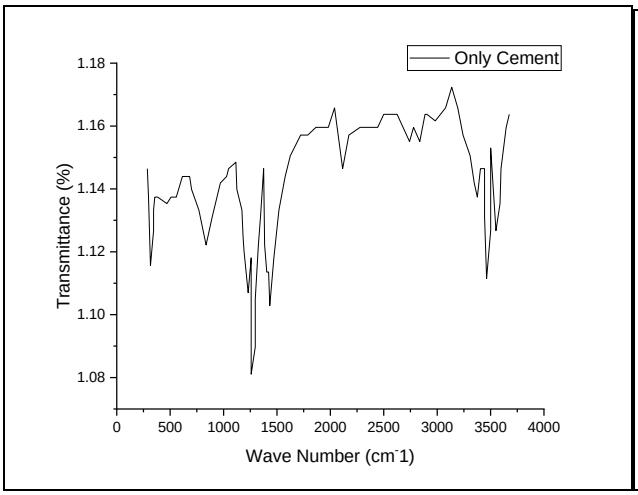

Figure 17: FTIR graph for cementitious material

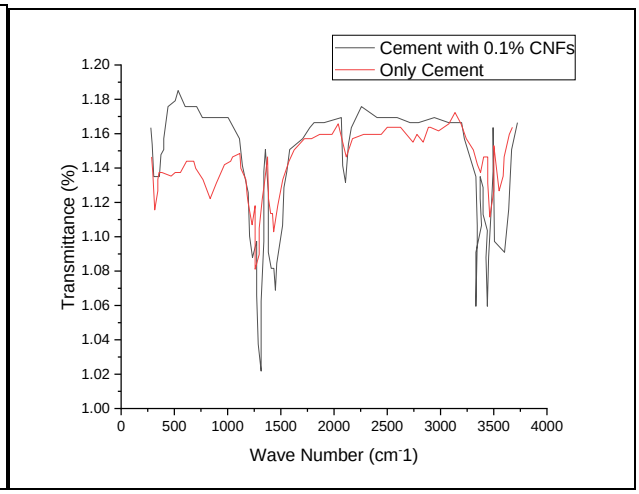

Figure 18: FTIR graph for cementitious material with 0.1% CNF

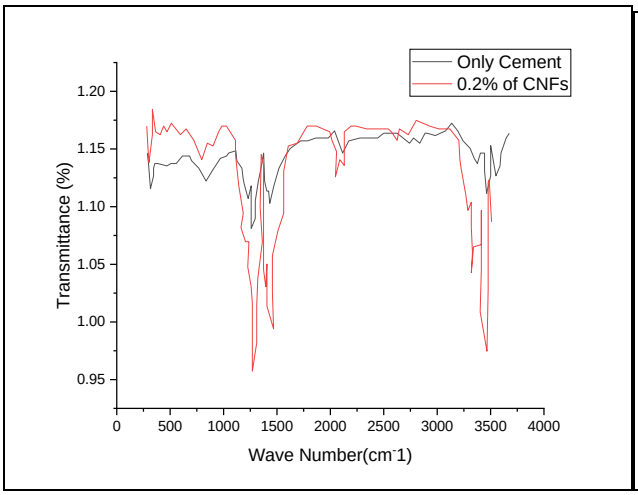

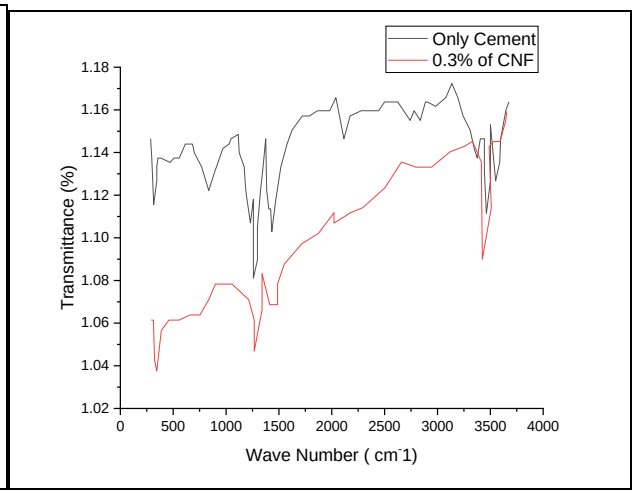

Figure 19: FTIR graph for with 0.2% and 0.3% CNFs introduced in cementitious material

symmetric and irregular stretching of the O-H vibrator of the water molecules.The remaining fig gives the comparison with and without CNFs(various percentages) in a cementitious material. The detectable broad peaks of fig 18 at

1115,1375,2039,2278,2499,2886,3136 cm-1 suggest the presence of some organic functional groups, such as C-O, O-H, and carboxyl groups, which could enable the adsorption of aniline via hydrogen bond. Fig 19 shows the FTIR graph for 0.2% and 0.3% CNFs introduced in cementitious material that detects the board peaks of 1352, 1457, 1738, 2194, 2803, and 1340, 2020, 2660 3331, respectively. This peak was correlated with the spectroscopy table, which attributed to the Benzenoid rings' C = O and C-H stretching vibration mode, the widening mode of C-N, and the protonated C-N group, respectively. Figures 18 and 19 also show that introducing various percentage CNFs gives increasing intensities of most peaks of the cementitious material compared with normal cementitious material. It indicates that polymer adhesionwith CNFs was good, and it leads to the restricted motion of the molecular chains. These interactions may enableelectron delocalization which increasesbonding between cementitious material and CNFs.

Conclusion:

In this paper, various percentagesof CNF were mixed as a reinforcement withthe cement matrix. Multiple sets of the beam and cube were prepared to examine the rheological properties of cementitious material. There was three no of the beam/cube cast in every set, and the average results were taken from these. 3 point flexural strength test and compressive strength were tested.Transmission electron microscope (TEM) imageswere usedto calculate the sonicatedtime inthe ultrasonic mixture for the different types of sample, whether it was dispersed correctly or not. After getting proper sonicated time, an aqueous solution was prepared to disperse the CNF. An ultrasonic mixer was used to disperse the solution, and then it was mixed with cement,keepinga 0.4 water-cement ratio. Cubes were prepared to find out the compressive strength, and the beam was prepared to find out the flexural strength on 7, 14, and 28 days. It was detected that the peak load of the compressive strength test was increased with an increase inthe percentage of CNFs with cement. After 28 days, the peak load was increased by 76 %,increasingthe carbon nanofibers' percentage. SEM result of all sample was also made to know the proper bonding between nanofiber and cementitious material, and XRD results give the peaks result as well as crystalline size and index.

1. TEM results showed that increasing sonicated time in ultrasonic mixture dispersion rate of nanofiber was also growing. After multiple tests, 30 min sonication time was considered for better dispersion results.
2. After sonication and proper mixing beam sample were prepared for the 3-point bending strength test, it was observed that for large beam and small types of a beam, an increase of the percentage of CNF, the flexural strength was increased by 43%, 65%, and 68%.

3. The modulus of elasticity and toughness had also carried out and observed that incresing of nanofiber percentage the variation was 22%,36% and 66% respectively. In the case of toughness initially increses but after some percentage it was decrease.
4. SEM images were also observed, and it was verified that due to poor dispersion, some microcracks were generated. The fibers pull-out was introduced for the weaker bonding between CNF and cement matrix.
5. The XRD analysis confirms the formation of more C-S-H in CNF cementitious material. Due to the increase of FWHM and peak value, CNF gives more strength and increases the bonding between two materials.
6. The crystallinity index were increased by 20%,29% and 41%(E. Cristiano, 2011) as increase the percentage of CNF (0.1%,0.2%,0.3%) in cementitious material.
7. Detectable board peaks of FTIR spectroscopy result also shows the molecular bonding between the cementitious material and the various percentage of CNFs.

Conflict of interest statement: On behalf of all authors, the corresponding author states no conflict of interest.

References

Bryan M. Tyson, S.M.ASCE; Rashid K. Abu Al-Rub, M.ASCE; Ardavan Yazdanbakhsh, S.M.ASCE; and Zachary Grasley, M.ASCE. (2011). Carbon Nanotubes and Carbon Nanofibers for Enhancing the Mechanical Properties of Nanocomposite Cementitious Materials. *American Society of Civil Engineers*, 1028-1035. doi:10.1061/(ASCE)MT.1943-5533.0000266.

D. J. Bannwaster, G. R. Davies, I. M. Ward, and J. F. McIntyre. (1984). Ionic conductivities of poly(methoxy polyethylene glycol monomethacrylate. *Polymer, 25*, 1600-1602.

Mejdoub R, Hammi H, Sunol J, Boufi S. (2016). "Nanofibrillated cellulose as nano reinforcement in Portland cement: Thermal, mechanical and microstructural properties. *Journal of Composite Materials*, 51(17). doi:10.1177/0021998316672090

Nur Yazdani, Vinoth Mohanam. (2014, June). Carbon Nano-Tube and Nano-Fiber in Cement Mortar: Effect of Dosage Rate and Water-Cement Ratio. *International Journal of Material Science (IJMSCI), Volume 4* (issue 2). doi:10.14355/ijmsci.2014.0402.01

S. R. Dhakate et al. (2016). Excellent mechanical properties of carbon fiber semi-aligned electrospun carbon nanofiber hybrid polymer composites. *Royal Society Of chemistry advances.*

Mohammed H. Al-Saleh, Uttandaraman Sundararaj. (3. December 2011). 3. Review of the mechanical properties of carbon nanofiber/polymer composites. *3. Composites Part A: Applied Science and Manufacturing*, Pages 2126-2142. doi:https://doi.org/10.1016/j.compositesa.2011.08.005

Mohammed H. Al-Saleh, Uttandaraman Sundararaj. (January 2009). A review of vapor grown carbon nanofiber/polymer conductive composites. *A review of vapor grown carbon nanofiber/polymer conductive composites*, Pages 2-22, doi:https://doi.org/10.1016/j.carbon.2008.09.039

Altoubat, S. Y.-A. (2009). Shear behavior of macro-synthetic fiber-reinforced concrete beams without stirrups.*ACI Mater. J., 106*(4), 381–389.

Coleman, J. N. (2006). Small but strong: A review of the mechanical properties of carbon nanotube-polymer composites. *Carbon, 44*(9), 1624–1652.

Das, K. &. (2010). Study of the Properties of Microcrystalline Cellulose Particles from Different Renewable Resources by XRD, FTIR, Nanoindentation, TGA, and SEM. *Journal of Polymers and the Environment*.

Das, K. R. (2009). A study of the mechanical, thermal, and morphological properties of microcrystalline cellulose particles prepared from cotton slivers using different acid concentrations. *Cellulose*(16(5)), 783-793. doi:https://doi.org/10.1007/s10570-009-9280-6

Du, X. L. (2012). Use of facile mechanochemical method to functionalize carbon nanofibers with nanostructured polyaniline and their electrochemical capacitance. ,. *Nanoscale Res Lett 7, 111*. DOI: https://doi.org/10.1186/1556-276X-7-111

E. Crwastiano, Y.-J. H. (2011). A comparison of point of zero charge measurement methodology. *Clays and Clay Minerals, vol. 59,* (no. 2,), 107–115,

Fwascher, G., and Li, V. C. (2007). Effect of fiber reinforcement on the response of structural members. *Eng. Fract. Mech., 74(1–2),* 258–272.

Gea, S. S.-A. (2020). Wasolation and Characterwasation of Cellulose Nanofibre and Lignin from Oil Palm Empty Fruit Bunches. *Materials (Basel, Switzerland), 13(10): 2290.* doi:10.3390/ma13102290

Grunlan, C. L. (2008). Weak polyelectrolyte control of carbon nanotube dispersion in water. *J. Colloid Interface Sci, 317(1),* 346–349.

I. Teng, H. H. (2012). Fabrication of cone-shaped CNF/SiC-coated Si-nanocone composite structures and their excellent field emission performance. *Nanoscale, 7362*(4). DOI: 10.1039/C2NR31511D

Li, G. Y., Wang, P. M., and Zhao, X. (2005). Mechanical behavior and microstructure of cement composites incorporating surface-treated multi-walled carbon nanotubes. *Carbon, 43*(6), 1239–1245.

Mejdoub R et.al. (2016). Nanofibrillated cellulose as nano reinforcement in Portland cement: Thermal, mechanical and microstructural properties. *Journal of Composite Materials, 51*(17). DOI: 10.1177/0021998316672090

Mir Mohammad Alavi Nikje, M. N. (2008, September 1). Microwave-aswasted Polyurethane Bond Cleavage via Hydroglycolyswas Process at Atmospheric Pressure. *44*(5), 367-380. doi:https://doi.org/10.1177/0021955X08090279

Mondragon, G. &. (2014). A common strategy to extracting cellulose nanoentities from different plants. *Industrial Crops and Products, 55,* 140–148.

Panel Muneer et al. (2015, December 5). Optimization of nickel oxide nanoparticle synthesis through the sol-gel method using Box–Behnken design. *Materials & Design, Volume 86,* Pages 948-956. doi:https://doi.org/10.1016/j.matdes.2015.07.176

Scalwasi, F. (2009). *Nanostructured Materials in New and Exwasting Buildings: To Improved Performance and Saving Energy*. Berlin Heidelberg: Springer, Berlin, Heidelberg. doi:https://doi.org/10.1007/978-3-642-00980-8_47

Thien Duc Nguyen Van, S. S. (2014). Characterization of Carbon Nanofibers Treated with Thermal Nitrogen as a Catalyst Support Using Point-of-Zero Charge Analyswas. *Journal of Nanomaterials, vol. 2014*(Article ID 631069). doi:https://doi.org/10.1155/2014/631069

Viet, D. B.-C. (2007). Dwaspersion of cellulose nanocrystals in polar organic solvents. *Cellulose, 14,* 109–113. doi:https://doi.org/10.1007/s10570-006-9093-9

Yazdanbakhsh, A., Grasley, Z., Tyson, B., and Abu Al-Rub, R. (2009). Carbon nanofibers and nanotubes in cementitious materials: Some issues. *Special Publication V, ACI, MI, SP 267*, 21–34.

Yazdani, Nur & Mohanam, Vinoth. (2014). Carbon Nano-Tube and Nano-Fiber in Cement Mortar: Effect of Dosage Rate and Water-Cement Ratio. *International Journal of Material Sciences, 4,* 45. doi:10.14355/ijmsci.2014.0402.01

Yehya M. Ahmed, A. A.-M. (2016). Syntheses and Characterization of Carbon Nanofibers Grown on Powdered Activated Carbon. *Journal of Nanotechnology, Article ID 15*, 10 pages, doi:https://doi.org/10.1155/2016/1538602

Zhengping Zhoua, Chuilin Laia,b, Lifeng Zhangb, Yong Qiana, Haoqing Houa, Darrell H. Renekerc, Hao Fongb,(2009). Development of carbon nanofibers from aligned electrospun polyacrylonitrile nanofiber bundles and characterization of their microstructural, electrical, and mechanical properties. *Polymer*, 2999–30063000. DOI:10.1016/j.polymer.2009.04.058